Inorganic Chemistry

ARTICLE

pubs.acs.org/IC

Syntheses, Structures, and Magnetic Properties of a Family of Tetra-, Hexa-, and Nonanuclear Mn/Ni Heterometallic Clusters

Hui Chen, Cheng-Bing Ma, Da-Qiang Yuan, Ming-Qiang Hu, Hui-Min Wen, Qiu-Tian Liu, and Chang-Neng Chen*

State Key Laboratory of Structural Chemistry, Fujian Institute of Research on the Structure of Matter, The Chinese Academy of Sciences, Fuzhou, Fujian 350002, China

Supporting Information

ABSTRACT: A family of Mn^{III}/Ni^{II} heterometallic clusters, $[Mn^{III}_4Ni^{II}_5(OH)_4(hmcH)_4(pao)_8Cl_2]\cdot 5DMF$ (**1**·5DMF), $[Mn^{III}_3Ni^{II}_6(N_3)_2(pao)_{10}(hmcH)_2(OH)_4]Br\cdot 2MeOH\cdot 9H_2O$ (**2**·2MeOH·9H$_2$O), $[Mn^{III}Ni^{II}_5(N_3)_4(pao)_6(paoH)_2(OH)_2](ClO_4)\cdot MeOH\cdot 3H_2O$ (**3**·MeOH·3H$_2$O), and $[Mn^{III}_2Ni^{II}_2(hmcH)_2(pao)_4(OMe)_2(MeOH)_2]\cdot 2H_2O\cdot 6MeOH$ (**4**·2H$_2$O·6MeOH) [paoH = pyridine-2-aldoxime, $hmcH_3$ = 2, 6-Bis(hydroxymethyl)-*p*-cresol], has been prepared by reactions of Mn(II) salts with $[Ni(paoH)_2Cl_2]$, $hmcH_3$, and NEt_3 in the presence or absence of NaN_3 and characterized. Complex **1** has a $Mn^{III}_4Ni^{II}_5$ topology which can be described as two corner-sharing $[Mn_2Ni_2O_2]$ butterfly units bridged to an outer Mn atom and a Ni atom through alkoxide groups. Complex **2** has a $Mn^{III}_3Ni^{II}_6$ topology that is similar to that of **1** but with two corner-sharing $[Mn_2Ni_2O_2]$ units of **1** replaced with $[Mn_3NiO_2]$ and $[MnNi_3O_2]$ units as well as the outer Mn atom of **1** substituted by a Ni atom. **1** and **2** represent the largest 3d heterometal/oxime clusters and the biggest $Mn^{III}Ni^{II}$ clusters discovered to date. Complex **3** possesses a $[MnNi_5(\mu\text{-}N_3)_2(\mu\text{-}OH)_2]^{9+}$ core, whose topology is observed for the first time in a discrete molecule. Careful examination of the structures of **1**−**3** indicates that the Mn/Ni ratios of the complexes are likely associated with the presence of the different coligands $hmcH^{2-}$ and/or N_3^-. Complex **4** has a $Mn^{III}_2Ni^{II}_2$ defective double-cubane topology. Variable-temperature, solid-state dc and ac magnetization studies were carried out on complexes **1**−**4**. Fitting of the obtained $M/(N\mu_B)$ vs H/T data gave $S = 5$, $g = 1.94$, and $D = -0.38$ cm^{-1} for **1** and $S = 3$, $g = 2.05$, and $D = -0.86$ cm^{-1} for **3.** The ground state for **2** was determined from ac data, which indicated an $S = 5$ ground state. For **4**, the pairwise exchange interactions were determined by fitting the susceptibility data vs T based on a 3-J model. Complex **1** exhibits out-of-phase ac susceptibility signals, indicating it may be a SMM.

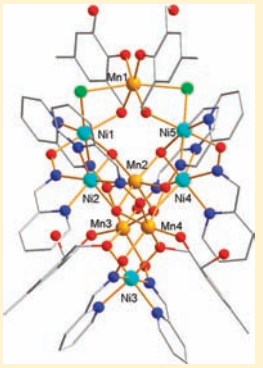

INTRODUCTION

The synthesis and study of polynuclear 3d metal clusters have been attracting intense interest in the past 20 years. This is mainly due to the relevance of this type of species to biological system[1] and molecular magnetism,[2] as well as to their aesthetically beautiful structures. Some of these complexes possess high-spin ground states and easy-axis-type magnetic anisotropy, resulting in a significant energy barrier to reversal of the magnetization vector and functioning as "single molecular magnets" (SMMs).[3] SMMs are of particular interest in physics, chemistry, and materials science because of their fundamental properties, such as quantum phenomena, finite-size effects, and potential applications in magnetic devices. To date, the majority of SMMs have been found among homometallic Mn clusters containing Mn(III) atoms,[4] which is because such clusters often have large spin ground states as well as large negative magnetoanisotropy associated with the presence of Jahn−Teller-distorted Mn(III) atoms. On the other hand, by incorporating heterometal spins, it is possible to affect the spin ground state, magnetic anisotropy, and magnetic exchange interactions within SMMs. In this regard, considerable efforts have also been made to develop heterometallic species for seeking new routes to distinctly different properties.[5]

The oxime ligands are well known for their propensity to form polynuclear complexes, both homo- and heteronuclear. Activation of oximes by 3d transition metals toward polynuclear compounds with various architectures and interesting magnetic properties is becoming a fruitful area of research,[6] among which some of the compounds have been recently found to exhibit single-molecule magnetism[7] or single-chain magnetism[8] behavior. So far, a number of 3d homometallic clusters with oxime ligands have been prepared,[9] with nuclearities ranging from 3 to 14. However, their heteropolynuclear analogues are limited to those with low nuclearities,[6a,b,10] most of which are di-, tri-, or tetranuclear complexes, with a hexanucluear $Mn^{III}_4Ni^{II}_2$ compound[10f] being the highest one. Searching for higher nuclearity heterometallic clusters would be interesting as they may present distinctly different architectures and magnetic properties compared with the homometallic ones.

The strategy of using "metal oximates" as ligands has proven successful in preparing the metal/oxime clusters. Various "metal oximates" have been used as building blocks, such as $[NaFe(RL)_3]\cdot H_2O$ (RL^- = ary1azo oximate),[11] $[Cu(DopnH)]^+$

Received: July 1, 2011
Published: September 16, 2011

Scheme 1. Structural Formula of Pyridine-2-aldoxime and 2,6-Bis(hydroxymethyl)-*p*-cresol (top), and Coordination Modes of the pao^-, $hmcH^{2-}$, and N_3^- Ligands Present in Complexes 1−4 (bottom)

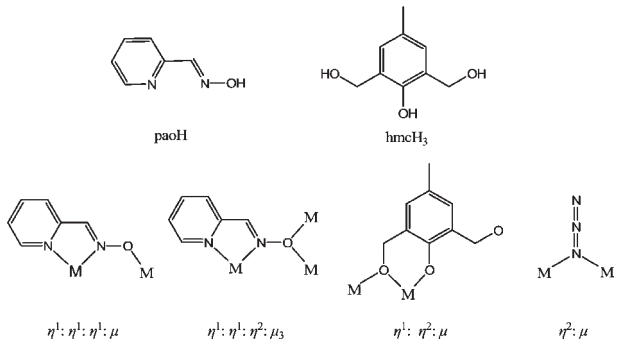

(H_2Dopn =3,9-dimethyl-4,8-diazaundeca-3,8-diene-2,10-dione dioxime),[12] $[Ni(pao)_2(py)_2]$ (pao^- = pyridine-2-aldoximate),[8a,b,10f] $[M(PyA)_3]^{n-}$ (M = certain 3d metal, PyA^- = pyridine-2-aldoximate),[10g,13] and $[Cu(DapdoH_2)_2]^{2+}$ ($Dapdo^{2-}$ = 2,6-diacetylpyridine dioximate).[14] However, most of the "metal oximates" building blocks used previously contain only the coordinating functional groups, namely, the oximate coordination donors. Here, we attempt to use $[Ni(paoH)_2Cl_2]$,[15] a "metal oximate" containing both coordinating functional groups and exchangeable terminal ligands, as the building block. In addition to the pair of oximate coordination donors, $[Ni(paoH)_2Cl_2]$ also possesses two exchangeable terminal Cl^- ligands, which could be easily replaced by other bridging groups potentially functioning as magnetic pathways between magnetic centers. By introducing the coligands NaN_3 and 2,6-bis(hydroxymethyl)-*p*-cresol ($hmcH_3$) (Scheme 1), the latter of which has been used sparingly in manganese cluster chemistry,[16] together with the metalloligand $[Ni(paoH)_2Cl_2]$, we obtain a family of Mn^{III}/Ni^{II} heterometallic clusters with various nuclearities: $[Mn^{III}_4Ni^{II}_5(OH)_4(hmcH)_4(pao)_8Cl_2]\cdot 5DMF$ (**1**·5DMF), $[Mn^{III}_3Ni^{II}_6(N_3)_2(pao)_{10}(hmcH)_2(OH)_4]Br\cdot 2MeOH\cdot 9H_2O$ (**2**·2MeOH·9H_2O), $[Mn^{III}Ni^{II}_5(N_3)_4(pao)_6(paoH)_2(OH)_2](ClO_4)\cdot MeOH\cdot 3H_2O$ (**3**·MeOH·3H_2O), and $[Mn^{III}_2Ni^{II}_2(hmcH)_2(pao)_4(OMe)_2(MeOH)_2]\cdot 2H_2O\cdot 6MeOH$ (**4**·2H_2O·6MeOH).

The syntheses, structures, and magnetochemical characterizations of these complexes are described in this paper. To our knowledge, **1** and **2** are the largest 3d heterometal/oxime clusters and the biggest $Mn^{III}Ni^{II}$ clusters discovered to date.

EXPERIMENTAL SECTION

Syntheses. All reagents are of commercially available analytical reagent grade and were used without further purification. $[Ni(paoH)_2Cl_2]$ was prepared according to the literature method.[15] WARNING: Azido and perchlorate salts are potentially explosive; such compounds should be used in small quantities and handled with caution.

$[Mn^{III}_4Ni^{II}_5(OH)_4(hmcH)_4(pao)_8Cl_2]\cdot 5DMF$ (1·5DMF). To a stirred green solution of $[Ni(paoH)_2Cl_2]$ (0.19 g, 0.5 mmol), $MnCl_2\cdot 4H_2O$ (0.1 g, 0.5 mmol), and $hmcH_3$ (0.084 g, 0.5 mmol) in DMF (10 mL) was added NEt_3 (0.56 mL, 4 mmol). The resulting dark solution was stirred for 30 min and filtered. The filtrate was layered with Et_2O/hexane (15 mL, 1:1 v/v) for 2 weeks to deposit black crystals of **1**·5DMF in ∼47% yield. Anal. Calcd (found) for **1** (solvent free): C, 44.14 (43.72); H, 3.70 (4.11); N, 9.80 (9.60). Selected IR data (KBr, cm^{-1}): 3413 (mb), 1650 (m), 1604 (s), 1524(w), 1472 (s), 1258 (m), 1224 (w), 1159 (w), 1122 (s), 1078 (s), 1017 (w), 811 (m), 733 (m), 643 (m).

$[Mn^{III}_3Ni^{II}_6(N_3)_2(pao)_{10}(hmcH)_2(OH)_4]Br\cdot 2MeOH\cdot 9H_2O$ (2·2MeOH·9H_2O). To a stirred light brown solution of $[Ni(paoH)_2Cl_2]$ (0.19 g, 0.5 mmol), $Mn(OAc)_2\cdot 4H_2O$ (0.24 g, 1 mmol), and $hmcH_3$ (0.084 g, 0.5 mmol) in MeOH/DMF (15/1 mL) were added NEt_3 (0.56 mL, 4 mmol) and solid NaN_3 (0.65 g, 1 mmol). The resulting dark brown suspension was stirred for 4 h before NBu_4Br (0.32 g, 1 mmol) was added. After stirring for another 30 min, the suspension was filtered and the filtrate was left undisturbed at room temperature for 2 weeks to give black crystals of **2** mixed with crystals of a known[13] cluster $[Ni(Pao)_3Mn(Pao)_3Ni]^+$. **2** was separated by recrystallization of the products from MeOH. Anal. Calcd (found) for **2** (solvent free): C, 40.87 (40.39); H, 3.25 (3.59); N, 15.89 (15.47). Selected IR data (KBr, cm^{-1}): 3410 (mb), 2069 (s), 1653 (w), 1602 (s), 1524 (m), 1473 (s), 1220 (m), 1117 (s), 1093 (s), 779 (m), 687 (m).

$[Mn^{III}Ni^{II}_5(N_3)_4(pao)_6(paoH)_2(OH)_2](ClO_4)\cdot MeOH\cdot 3H_2O$ (3·MeOH·3H_2O). To a stirred white suspension of ammonium triacetic acid (0.095 g, 0.5 mmol), $Mn(ClO_4)_2\cdot 6H_2O$ (0.18 g, 0.5 mmol), and NaN_3 (0.97 g, 1.5 mmol) in MeOH (15 mL) was added a green solution of $[Ni(paoH)_2Cl_2]$ (0.19 g, 0.5 mmol) in DMF (5 mL). The resulting brown solution was added NEt_3 (0.56 mL, 4 mmol) and stirred for a further 30 min and filtered. The filtrate was left undisturbed at room temperature for 2 months to deposit dark brown crystals of **3** in ∼20% yield. Anal. Calcd (found) for **3** (solvent free): C, 35.57 (35.23); H, 2.74 (2.97); N, 24.20 (23.90). Selected IR data (KBr, cm^{-1}): 3444 (mb), 2063 (s), 1602 (m), 1536 (w), 1474 (m), 1110 (m), 1082 (s), 776 (w), 683 (w).

$[Mn^{III}_2Ni^{II}_2(hmcH)_2(pao)_4(OMe)_2(MeOH)_2]\cdot 2H_2O\cdot 6MeOH$ (4·2H_2O·6MeOH). Complex **4**·2H_2O·6MeOH was prepared in the same manner as complex **1** but using MeOH in place of DMF. The filtrate was left undisturbed at 4 °C for 2 weeks to deposit black needle-like crystals in ∼33% yield. Anal. Calcd (found) for **4** (solvent free): C, 47.21 (46.72); H, 4.65 (4.51); N, 9.58 (9.40). Selected IR data (KBr, cm^{-1}): 3419 (mb), 2921 (m), 2819 (m), 1603 (s), 1539 (w), 1470 (s), 1255 (m), 1222 (w), 1114 (m), 1091 (s), 1015 (m), 700 (m), 604 (w).

Physical Measurements. Elemental analyses were carried out on a Vario EL III Elemental Analyzer. IR spectra were recorded on a Magna-75 FT-IR spectrometer using KBr pellets in the range of 4000−400 cm^{-1}. Variable-temperature dc and ac susceptibility magnetic data for complexes **1**−**4** were measured on a PPMS-9T superconducting magnetometer employing the dried and finely ground polycrystalline samples kept in a capsule. Diamagnetic corrections were made with Pascal's constants for all the constituent atoms of the complexes.

X-ray Crystallography. X-ray single-crystal data of complexes **1**−**4** were collected on a Saturn 70 diffractometer with Mo Kα radiation (λ = 0.71073 Å) using an ω-scan mode. The program SADABS[17] was used for absorption correction. The structures were solved by direct methods and refined by full-matrix least-squares techniques using the SHELXTL-97[18] program package. All non-hydrogen atoms were refined anisotropically. Hydrogen atoms were determined with geometrical calculations riding on the related atoms, and their positions and thermal parameters were fixed during structure refinement. The solvent molecules of complex **1** are disordered and treated using the SQUEEZE[19] option in PLATON. Selected crystallographic data and refinement details for complexes **1**−**4** are displayed in Table 1.

RESULTS AND DISCUSSION

Synthesis. Reactions of the "metal oximate" $[Ni(paoH)_2Cl_2]$ and the coligands $hmcH_3$ and/or NaN_3 with manganese(II) salts in the presence of the base lead to a family of Mn^{III}/Ni^{II}

Table 1. Selected Crystallographic Data and Refinement Details for 1·5DMF, 2·2MeOH·9H_2O, 3·MeOH·3H_2O, and 4·2H_2O·6MeOH

	1·5DMF	2·2MeOH·9H_2O	3·MeOH·3H_2O	4·2H_2O·6MeOH
formula[a]	$C_{99}H_{119}Cl_2Mn_4N_{21}Ni_5O_{29}$	$C_{80}H_{100}BrMn_3N_{26}Ni_6O_{31}$	$C_{49}H_{54}ClMnN_{28}Ni_5O_{18}$	$C_{52}H_{82}Mn_2N_8Ni_2O_{22}$
fw, g mol^{-1}	2651.27	2518.68	1707.14	1398.56
cryst syst	triclinic	monoclinic	monoclinic	monoclinic
space group	*P*-1	*C*2/*c*	*C*2/*c*	*P*2(1)/*n*
a, Å	16.097(4)	17.9792(14)	37.188(9)	9.092(4)
b, Å	18.556(5)	15.5876(11)	16.461(4)	17.554(7)
c, Å	22.290(6)	35.996(3)	24.156(6)	18.843(8)
α, deg	109.646(2)	90.00	90.00	90.00
β, deg	98.1000(10)	103.096(4)	112.829(4)	102.304(7)
γ, deg	108.283(3)	90.00	90.00	90.00
V, Å ^{3}	5724(3)	9825.6(13)	13629(5)	2938(2)
Z	2	4	8	2
T, K	123.1500	113.1500	150.1500	150.1500
ρ_{calcd}, g cm^{-3}	1.324	1.693	1.664	1.581
μ, mm^{-1}	1.342	1.994	1.660	1.137
F(000)	2324	5092	6960	1464
R_1[b]	0.0649	0.0731	0.0650	0.0688
wR_2[c]	0.1878	0.2112	0.1700	0.1890

[a] Including solvent molecules. [b] $R_1 = \Sigma(||F_o| - |F_c||)/\Sigma|F_o|$. [c] $wR_2 = [\Sigma w(F_o^2 - F_c^2)^2/\Sigma w(F_o^2)^2]^{0.5}$.

Scheme 2. Synthesis of Complexes 1−4

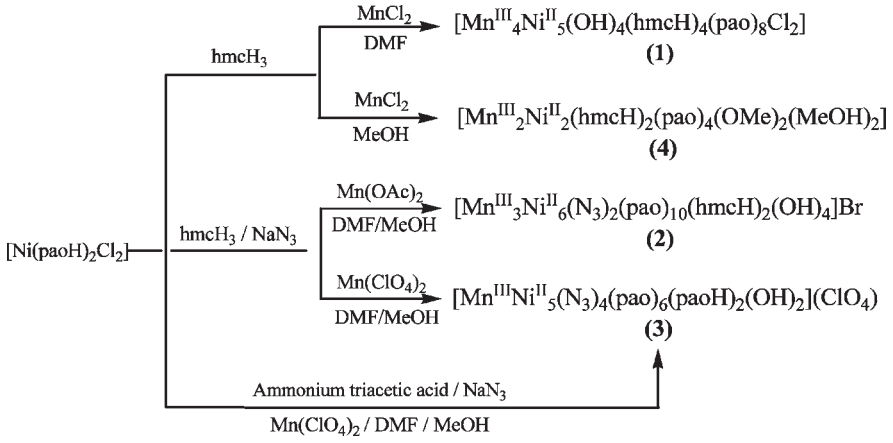

heterometallic clusters ranging in nuclearity from four to nine. The synthetic routes and products obtained are shown in Scheme 2. $HmcH_3$ was selected as one of the coligands because it has three potential O donors which could give rise to a variety of coordination modes and probably provide an effective magnetic pathway between the metal atoms as well as this ligand has not been fully explored. NEt_3 acts as the base to facilitate both deprotonation of the oxime and $hmcH_3$ ligands and air oxidation of the Mn(II) starting material, since it is well known that higher pH values favor formation of Mn(III) ions.

The first obtained complex is the tetranuclear **4** with a $Mn^{III}_2Ni^{II}_2$ topology, which was prepared by reaction of $[Ni(paoH)_2Cl_2]$ with $MnCl_2·4H_2O$ and $hmcH_3$ in MeOH in the presence of NEt_3. However, the same reaction carried out in DMF gave **1**, a nonanuclear cluster with a $Mn^{III}_4Ni^{II}_5$ topology, suggesting that the reaction products are solvent dependent, as is often seen in the transition metal cluster chemistry.

Since the structures of **1** and **4** reveal the presence of bridging hydroxide/methoxide groups, it is expected that adding NaN_3 to the reaction system may foster formation of clusters with higher ground-state spin values if the hydroxide/methoxide bridges are replaced by the end-on N_3^- bridges. As expected, reactions of $[Ni(paoH)_2Cl_2]$ with Mn(II) salts, $hmcH_3$, and NaN_3 in the presence of NEt_3 gave two new clusters with end-on N_3^- bridges within them, but unexpectedly, the N_3^- bridges substitute for the alkoxide bridges of the $hmcH^{2-}$ ligands other than the hydroxide/methoxide bridges. The nonanuclear **2** with a $Mn^{III}_3Ni^{II}_6$ topology and the hexanuclear **3** with a $Mn^{III}Ni^{II}_5$ topology are structurally related to complex **1**, containing similar units that clearly distinguish **1**−**3** from **4**. Careful examination of the structures of **1**−**3** indicates that the Mn/Ni ratios of the complexes are likely influenced by the presence of the ancillary ligands $hmcH^{2-}$ and/or N_3^-.

dx.doi.org/10.1021/ic201403k |*Inorg. Chem.* 2011, 50, 10342–10352

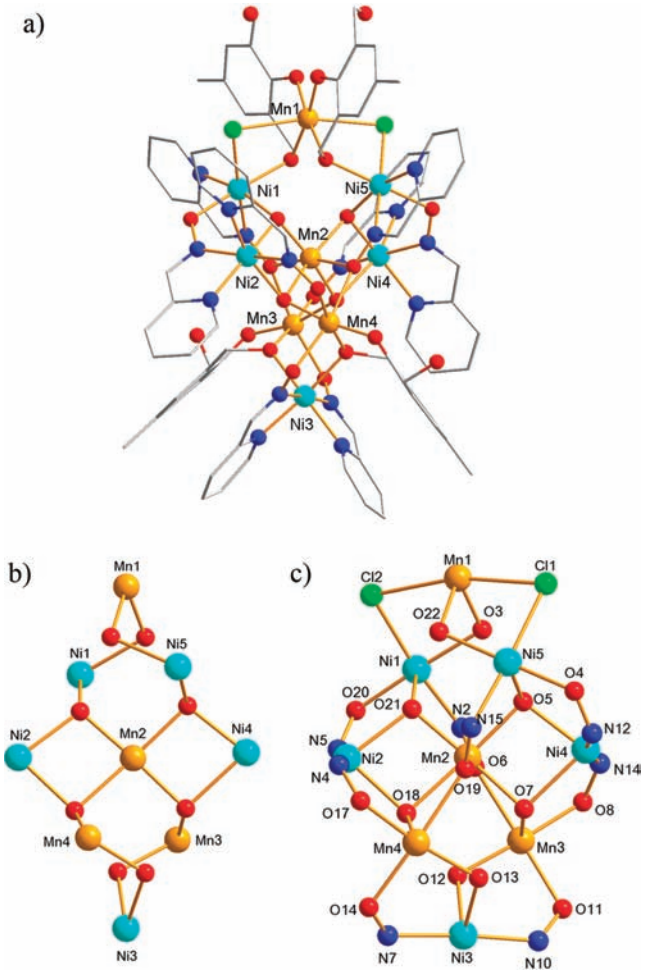

Figure 1. (a) Structure of complex **1**. (b) Representation of the $[Mn^{III}_4Ni^{II}_5(\mu_3\text{-OH})_4(\mu\text{-OR})_4]^{10+}$ core of **1**. (c) Complete $[Mn^{III}_4Ni^{II}_5(\mu_3\text{-OH})_4(\mu\text{-OR})_4(\mu\text{-ON})_8(\mu\text{-Cl})_2]$ core. Color scheme: Mn, yellow; Ni, cyan; O, red; N, blue; C, gray; Cl, green. Hydrogen atoms have been omitted for clarity.

We also explored a variety of other reactant ratios for each system, most of which can afford the corresponding complex in varying yields, indicating that reactant ratio is not a key factor.

During the preparation of **2**, crystals of a known[13] cluster $[Ni(pao)_3Mn(pao)_3Ni]^+$ were presented together with **2**, which could not be eliminated by changing the synthetic conditions. Taking advantage of their different solubility in MeOH (**2** is well soluble, while the latter cluster is insoluble), we separated **2** from the known cluster by recrystallization of the products from MeOH.

A problem arising from the preparation of **3** is the low yield and presence of byproduct. Since its structure does not contain $hmcH_3$ ligand, we tried first to remove $hmcH_3$ from the reaction system but no isolable product was obtained. After several unsuccessful attempts, we finally established an alternative route to synthesize **3** in better yields and higher purity by using ammonium triacetic acid instead of $hmcH_3$.

Description of Crystal Structures. The structure of complex **1** is presented in Figure 1a, and selected interatomic distances and angles are listed in Table 2. Complex **1**·5DMF crystallizes in the triclinic space group *P*-1. Charge consideration, bond-valence-sum (BVS)[20] calculation, and the detection of Mn^{III} Jahn−Teller elongation axes indicate that **1** has four Mn^{III} atoms and five Ni^{II} atoms. The structure consists of a $[Mn^{III}_4Ni^{II}_5(\mu_3\text{-OH})_4(\mu_2\text{-OR})_4]^{10+}$ (RO^{2-} = $hmcH^{2-}$) core which can be described as two corner-sharing $[Mn_2Ni_2O_2]$ butterfly units (Mn2−Mn4−Ni2−Ni1 and Mn2−Mn3−Ni4−Ni5 related by four μ_3-OH) bridged to an additional Mn atom (Mn1) and a Ni atom (Ni3) through μ-alkoxo groups of the $hmcH^{2-}$ ligands (Figure 1b). The $hmcH^{2-}$ ligands coordinate in a $\eta^1{:}\eta^2{:}\mu$ fashion, with the phenoxide O atom bound terminally, one deprotonated alkoxide arm bridging two Mn atoms, and the other protonated alkoxide arm unbound. Peripheral ligation is provided by two Cl^- ions and eight pao^- ligands, where the oximate groups bridge in two distinct ways: six in the $\eta^1{:}\eta^1{:}\eta^1{:}\mu$ fashion and two (O6 and O19) in the $\eta^1{:}\eta^1{:}\eta^2{:}\mu_3$ fashion (Figure 1c). All Mn atoms are six coordinate with slightly distorted octahedral geometries. Except for Mn1, which is bound to an O_4Cl_2 donor set, the other Mn atoms are all bound to an O_6 set. All Ni atoms possess slightly distorted octahedral geometries in which Ni1 and Ni5 are bound to an O_3N_2Cl donor set and the other Ni atoms to an O_2N_4 set. The metal···metal distances range from 3.078(1) to 3.577(1) Å, the shortest two [3.078(1) Å (Ni4···Mn2) and 3.123(1) Å (Ni2···Mn2)] of which are via a pair of μ_3-OH bridges.

Complex **2**·2MeOH·9H_2O (Figure 2a) crystallizes in the monoclinic space group *C*2/*c*. The asymmetric unit consists of one-half of a $[Mn^{III}_3Ni^{II}_6(N_3)_2(pao)_{10}(hmcH)_2(OH)_4]^+$ cation and one-half of a Br^- anion, as well as several solvate molecules; the latter will not be further discussed. Selected interatomic distances and angles are listed in Table 3. Charge consideration and bond-valence-sum (BVS)[20] calculation indicate that **2** has three Mn^{III} atoms and six Ni^{II} atoms. The $[Mn^{III}_3Ni^{II}_6(\mu_3\text{-OH})_4(\mu\text{-OR})_2(\mu\text{-N}_3)_2]^{11+}$ (RO^{2-} = $hmcH^{2-}$) core consists of two corner-sharing butterfly units of $[MnNi_3O_2]$ and $[Mn_3NiO_2]$ (Mn1−Ni2−Ni3−Ni2A and Mn1−Mn2−Ni4−Mn2A related by four μ_3-OH^- ions) bridged to two outer Ni atoms (Ni1 and Ni1A) through end-on μ-N_3^- ligands and μ-alkoxo groups of the $hmcH^{2-}$ ligands (Figure 2b). Peripheral ligation is completed by 10 NO^- oximate groups, where the oximate groups also bridge in two ways: eight in the $\eta^1{:}\eta^1{:}\eta^1{:}\mu$ fashion and two (O9 and O9A) in the $\eta^1{:}\eta^1{:}\eta^2{:}\mu_3$ fashion (Figure 2c). All Mn atoms are six coordinated to an O_6 donor set with slightly distorted octahedral geometries. All Ni atoms possess distorted octahedral geometries, and the chromophores are $Ni1ON_5$, $Ni2O_3N_3$, and $Ni(3,4)O_2N_4$. The metal···metal separations range from 3.050(2) to 3.591(3) Å, the shortest two [3.050(2) Å (Ni3···Mn1) and 3.072(0) Å (Ni4···Mn1)] of which are via a pair of μ_3-OH groups.

The cluster of **2** is thus structurally similar to that of **1**, with the differences being (i) two corner-sharing butterfly units of $[Mn_3NiO_2]$ and $[MnNi_3O_2]$ in **2** versus two $[Mn_2Ni_2O_2]$ units in **1**, (ii) replacement of an outer Mn^{III} atom surrounded by two $hmcH^{2-}$ ligands and two Cl^- ligands in **1** by a Ni^{II} atom surrounded by two pao^- ligands, one N_3^- ligand, and one $hmcH^{2-}$ ligand in **2**, and (iii) replacement of one $hmcH^{2-}$ ligand which bridges the outer Ni^{II} atom and the butterfly units in **1** with one N_3^- ligand in **2**.

So far, there is a small family of nonanuclear metal/oxime clusters, of which are five Ni_9[9a,21a−c] clusters with a centered hexagonal bipyramid core of $[Ni_9(L)_{10}(\mu_3\text{-OH})_2(\mu_2\text{-OH})_2(\mu_2\text{-OH}_2)_2(H_2O)_6]^{4+}$ (L = pyridine-2-aldoximate or 1-methylimidazole-2-aldoxime) and a Mn_9[22] cluster $[Mn_9(\mu_4\text{-O})_2(\mu_3\text{-O})_4(CH_3CO_2)_4(pao)_8(paoH)_2]$ with a nearly planar core. Obviously, **1** and **2** are quite distinct from these clusters in structural topology besides participation of the coligand $hmcH_3$. **1** and **2** are the first

dx.doi.org/10.1021/ic201403k |*Inorg. Chem.* 2011, 50, 10342–10352

Table 2. Selected Interatomic Distances (Å) and Angles (deg) for Complex 1·5DMF

Mn1···Ni1	3.3370(11)	Ni1−Cl2	2.3710(12)	Ni4−N13	2.095(4)	Mn2−O7	1.988(3)
Mn1···Ni5	3.3209(12)	Ni2−N5	2.050(4)	Ni4−O7	2.261(3)	Mn2−O19	2.006(3)
Mn2···Ni1	3.3683(12)	Ni2−N4	2.059(4)	Ni5−O4	2.046(3)	Mn2−O5	2.062(3)
Mn2···Ni2	3.123(1)	Ni2−N6	2.077(4)	Ni5−N15	2.047(4)	Mn2−O18	2.171(3)
Mn2···Ni4	3.0781(10)	Ni2−N3	2.081(3)	Ni5−N16	2.092(4)	Mn3−O10	1.881(3)
Mn2···Ni5	3.4181(12)	Ni2−O18	2.120(3)	Ni5−O5	2.110(3)	Mn3−O12	1.931(3)
Mn2···Mn3	3.2181(11)	Ni2−O21	2.122(3)	Ni5−O22	2.130(3)	Mn3−O8	1.956(3)
Mn2···Mn4	3.3089(13)	Ni3−N10	2.031(3)	Ni5−Cl1	2.3831(14)	Mn3−O7	2.016(3)
Mn3···Ni3	3.4496(12)	Ni3−N7	2.046(4)	Mn1−O2	1.878(3)	Mn3−O11	2.131(3)
Mn4···Ni3	3.4132(10)	Ni3−N8	2.078(4)	Mn1−O23	1.892(3)	Mn3−O6	2.247(3)
Ni1···Ni2	3.5771(12)	Ni3−N9	2.096(4)	Mn1−O22	1.951(3)	Mn4−O16	1.875(3)
Ni4···Ni5	3.5368(10)	Ni3−O13	2.110(3)	Mn1−O3	1.958(3)	Mn4−O17	1.950(3)
Ni1−N2	2.024(4)	Ni3−O12	2.129(3)	Mn1−Cl2	2.6483(14)	Mn4−O13	1.967(3)
Ni1−O20	2.028(3)	Ni4−O5	2.043(3)	Mn1−Cl1	2.6744(15)	Mn4−O18	1.980(3)
Ni1−N1	2.093(4)	Ni4−N12	2.070(4)	Mn2−O21	1.925(3)	Mn4−O14	2.134(3)
Ni1−O21	2.135(3)	Ni4−N14	2.070(4)	Mn2−O6	1.978(3)	Mn4−O19	2.294(3)
Ni1−O3	2.145(3)	Ni4−N11	2.089(4)				
N1−Ni1−O21	164.98(13)	N8−Ni3−O13	167.49(13)	N15−Ni5−Cl1	176.76(10)	O12−Mn3−O8	176.28(14)
O20−Ni1−O3	176.93(12)	N9−Ni3−O12	164.80(12)	O2−Mn1−O22	173.78(14)	O10−Mn3−O7	165.88(14)
N2−Ni1−Cl2	173.68(10)	N12−Ni4−N14	165.31(14)	O23−Mn1−O3	173.34(15)	O11−Mn3−O6	166.73(12)
N5−Ni2−N4	167.82(13)	O5−Ni4−N11	156.69(14)	Cl2−Mn1−Cl1	166.96(4)	O17−Mn4−O13	172.79(13)
N3−Ni2−O18	160.86(13)	N13−Ni4−O7	156.90(14)	O21−Mn2−O7	170.11(12)	O16−Mn4−O18	172.51(13)
N6−Ni2−O21	161.11(13)	N16−Ni5−O5	164.49(14)	O6−Mn2−O19	163.41(13)	O14−Mn4−O19	164.49(12)
N10−Ni3−N7	175.39(15)	O4−Ni5−O22	178.95(12)	O5−Mn2−O18	164.14(11)		

heterometallic nonanuclear metal/oxime clusters discovered to date.

Complex **3**·MeOH·3H_2O crystallizes in the monoclinic space group *C*2/*c*. The asymmetric unit includes a $[Mn^{III}Ni^{II}_5(N_3)_4(pao)_6(paoH)_2(\mu_3\text{-}OH)_2]^+$ cation, a ClO_4^- anion, and several solvate molecules; the latter will not be further discussed. Selected interatomic distances and angles are listed in Table 4. The $1Mn^{III}$, $5Ni^{II}$ oxidation state situation of **3** was established by charge consideration, bond-valence-sum (BVS)[20] calculation, and detection of Mn^{III} Jahn−Teller elongation. The six metal atoms are held together by two μ_3-OH^- ions, four end-on bridging N_3^- ions, and six $\eta^1{:}\eta^1{:}\eta^1{:}\mu$ pao^- ligands. Peripheral ligation is completed by two chelating neutral paoH groups on Ni3 and Ni4 (Figure 3). The $[MnNi_5(\mu\text{-}N_3)_2(\mu_3\text{-}OH)_2]^{9+}$ core of the complex can be described as two corner-sharing $[Mn^{III}Ni^{II}_2(\mu_3\text{-}OH)]$ triangles (Mn1−Ni2−Ni3 and Mn1−Ni4−Ni5) bridged to an outer Ni^{II} (Ni1) atom through two N_3^- ions. The Mn^{III} atom has a slightly distorted octahedral geometry with the coordination environment defined by four oximate oxygen atoms and two hydroxo oxygen atoms, where one hydroxo oxygen and one oximate oxygen occupy the apical positions. All Ni^{II} atoms adopt slightly distorted octahedral geometries, with Ni(3,4) bound to an ON_5 donor set, Ni(2,5) to an N_4O_2 set, and Ni1 to an N_6 set. The distances between Mn^{III} and Ni^{II} atoms are 3.423(2) and 3.487(0) Å, respectively, while the separations among Ni^{II} atoms range from 3.124(2) to 3.475(2) Å, in which two monatomic bridges (μ_3-OH^- and μ-N_3^-) afford the shortest two [3.124(2) and 3.197(3) Å].

Complex **3** is the third member of the hexanuclear Mn/Ni clusters after complexes $Mn[Mn(hfac)_2]_3[Ni(pao)_3]_2$ ($hfac^-$ = hexafluoroacetylacetonate$^-$)[10f] and $[Mn_2Ni_4O_2(PhCOO)_{10}(DMF)_4]$.[23] The $[MnNi_5(\mu\text{-}N_3)_2(\mu_3\text{-}OH)_2]^{9+}$ topology in **3** is observed for the first time in a discrete molecule; however, it should be pointed out that it is similar to the fragments of two higher nuclearity Ni clusters previously reported,[9d] which are arranged as $[Ni_6(\mu\text{-}N_3)_2(\mu_3\text{-}OH)_2]^{8+}$.

Complex **4**·2H_2O·6MeOH crystallizes in the monoclinic space group $P2_1/n$, with the cluster lying on an inversion center. Selected interatomic distances and angles are listed in Table 5. The structure reveals the presence of Mn_2Ni_2 tetranuclear molecules. The metal atoms are located at the four corners of a defective face-sharing double cube and bridged by two μ_3-MeO^- groups, two NO^- oximate groups, and two μ-alkoxo groups of the $hmcH^{2-}$ ligands (Figure 4). The pao^- groups adopt a chelating mode and a $\eta^1{:}\eta^1{:}\eta^1{:}\mu$-bridging fashion, respectively. BVS calculations[20] and the presence of Jahn−Teller distortions suggest the Mn atoms to be trivalent. Each Mn atom has a slightly distorted octahedral geometry with the equatorial plane defined by the chelating $hmcH^{2-}$ group, an oximate O atom, and a methoxide μ_3-O atom. The apical positions are occupied by a terminal methoxide O atom and a methoxide μ_3-O atom. Each Ni^{II} atom adopts a slightly distorted octahedral geometry surrounded by two pao^- groups, one methoxide μ_3-O atom, and one alkoxide O atom of the $hmcH^{2-}$ ligand. The distance between Mn atoms is 3.355(1) Å, and the distances between Mn and Ni atoms are 3.104(5) (Mn1···Ni1) and 3.592(9) Å (Mn1′···Ni1).

4 joins a handful of Mn_2Ni_2 clusters, three of which possess a linear-type core[10e,24] and four have a defective double-cubane core.[5g,25] Compared with the defective double-cubane clusters previously reported, which contain only monatomic bridges between the metal centers, **4** has two NO bridges, and it is noteworthy that the Mn^{III} atoms in **4** are positioned in the central sites and the Ni^{II} atoms reside in both edges, is in contrast to the others.

Structural Correlation of Complexes 1−3. As shown in Figure 5, both structures of complexes **1** (Figure 5, bottom) and

dx.doi.org/10.1021/ic201403k |*Inorg. Chem.* 2011, 50, 10342–10352

2 (Figure 5, middle) contain the fragments of $[M_6(\mu_3\text{-OH})_2(\mu\text{-OR})_n(\mu\text{-N}_3)_{2-n}]$ which are similar to the core of complex **3** (Figure 5, top). Thus, the core of **1** and **2** can be seen as two torsionally fused $[M_6(\mu_3\text{-OH})_2(\mu\text{-OR})_n(\mu\text{-N}_3)_{2-n}]$ units sharing three common metal atoms. It was noticed that the bridging group of μ-OR^{2-} or μ-N_3^- is in close correlation with the presence of Mn or Ni atom. The presence of the Mn atom is concomitant with the μ-OR^{2-} group, and each μ-N_3^- group bridges two Ni atoms. This may originate from the different affinity of the metal atoms to the O or N donors. Thus, it is likely that the participation of the different coligands $hmcH^{2-}$ and/or N_3^- could affect the process of self-assembly and thus influence the Mn/Ni ratios of the complexes.

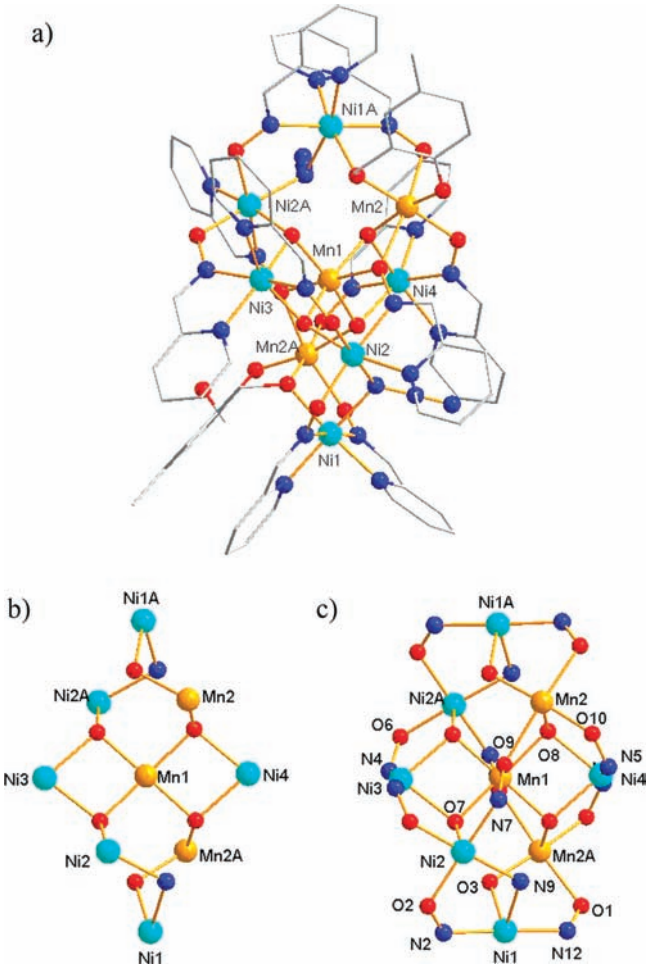

Figure 2. (a) Structure of complex **2**. (b) Representation of the $[Mn^{III}_3Ni^{II}_6(\mu_3\text{-OH})_4(\mu\text{-OR})_2(\mu\text{-N}_3)_2]^{11+}$ core of **2**. (c) Complete $[Mn^{III}_3Ni^{II}_6(\mu_3\text{-OH})_4(\mu\text{-OR})_2(\mu\text{-N}_3)_2(\mu\text{-ON})_{10}]^+$ core. Color scheme: Mn, yellow; Ni, cyan; O, red; N, blue; C, gray; Cl, green. Hydrogen atoms have been omitted for clarity.

Direct Current Magnetic Susceptibility Studies. The variable-temperature dc magnetic susceptibility data for **1**−**4** were collected in the temperature range 2.0−300 K in an applied field of 0.5 T. Plots of $\chi_m T$ vs T for complexes **1**−**3** are shown in Figure 6. The shapes of the curves are very similar, which decrease at first and then increase with decreasing temperature before a final drop at low temperature. This behavior indicates a mixture of both ferro- and antiferromagnetic exchange interactions within the complex, which is consistent with the presence of the bridging end-on azide groups/alkoxide groups and OH^-/oximate groups, since the former two typically give ferromagnetic interactions and the latter two typically give antiferromagnetic interactions. The final decrease at the lowest temperatures is assigned to Zeeman effects, zero-field splitting, and/or weak intermolecular interactions.

For **1**, the $\chi_m T$ value decreases slightly from 13.74 $cm^3\ K\ mol^{-1}$ at 300 K to reach a plateau in the 64−80 K region and then increases to a maximum of 14.16 $cm^3\ K\ mol^{-1}$ at 9.5 K before its final decrease down to 9.07 $cm^3\ K\ mol^{-1}$ at 2 K. The $\chi_m T$ value at 300 K is lower than the spin-only ($g = 2$) value of 17 $cm^3\ K\ mol^{-1}$ for four Mn^{III} and five Ni^{II} noninteracting ions, suggesting the presence of antiferromagnetic interactions. The maximum value at 9.5 K is close to the spin-only value expected for a complex with an $S = 5$ ground state (15 $cm^3\ mol^{-1}\ K$) with a g factor slightly less than 2.0. For **2**, the room-temperature $\chi_m T$ value is 14.97 $cm^3\ K\ mol^{-1}$, close to the spin-only ($g = 2$) value of 15 $cm^3\ K\ mol^{-1}$ for three Mn^{III} and six Ni^{II} noninteracting ions. The maximum value of 16.93 $cm^3\ K\ mol^{-1}$ at 28 K is close to the spin-only value expected for a complex with an $S = 5$ ground state with $g > 2$. Similar to that of **1**, the room-temperature $\chi_m T$ value (7.26 $cm^3\ K\ mol^{-1}$) for **3** is lower than the expected spin-only ($g = 2$) value of 8 $cm^3\ K\ mol^{-1}$ for one Mn^{III} and five Ni^{II} noninteracting ions. The maximum value at 18 K is 6.55 $cm^3\ K\ mol^{-1}$, close to the spin-only value expected for a complex with an $S = 3$ ground state (6 $cm^3\ mol^{-1}\ K$), with $g > 2$ as expected for Ni^{II} atoms in majority.

Table 3. Selected Interatomic Distances (Å) and Angles (deg) for Complex $2\cdot 2MeOH\cdot 9H_2O$

Ni1···Ni2	3.4681(9)	Ni1−N2	2.039(5)	Ni2−N8	2.102(5)	Mn1−O8	2.025(4)
Ni1···Mn2[a]	3.4109(11)	Ni1−N1	2.078(4)	Ni2−O7	2.106(3)	Mn1−O9	2.062(4)
Mn1···Ni2	3.3788(9)	Ni1−N13	2.089(5)	Ni3−N3	2.076(5)	Mn2−O4[a]	1.882(4)
Mn1···Ni3	3.0502(15)	Ni1−O3	2.110(3)	Ni3−N4	2.079(5)	Mn2−O3[a]	1.926(3)
Mn1···Mn2	3.2862(8)	Ni1−N9	2.122(4)	Ni3−O7	2.123(3)	Mn2−O10	1.936(4)
Mn1···Ni4	3.0720(15)	Ni2−O6[a]	1.990(4)	Ni4−N5	2.058(4)	Mn2−O8	2.053(3)
Ni2···Ni3	3.5913(9)	Ni2−O2	2.015(4)	Ni4−N6	2.088(4)	Mn2−O1[a]	2.139(4)
Mn2···Ni4	3.5583(9)	Ni2−N7	2.019(4)	Ni4−O8	2.122(3)	Mn2−O9	2.247(4)
Ni1−N12	2.036(5)	Ni2−N9	2.098(4)	Mn1−O7	1.973(3)		
N12−Ni1−N2	176.69(19)	O2−Ni2−N7	173.14(17)	N3[a]−Ni3−O7	156.93(17)	O9−Mn1−O9[a]	178.1(2)
N12−Ni1−N1	100.91(18)	O6[a]−Ni2−N9	178.12(16)	N5−Ni4−N5[a]	172.3(2)	O3[a]−Mn2−O10	175.20(16)
N13−Ni1−O3	167.04(17)	N8−Ni2−O7	167.13(17)	N6−Ni4−O8	158.53(15)	O4[a]−Mn2−O8	168.78(17)
N1−Ni1−N9	166.51(18)	N4[a]−Ni3−N4	166.2(3)	O7−Mn1−O8	166.43(14)	O1[a]−Mn2−O9	166.82(15)

[a] $-x + 1, y, -z + 1/2$.

dx.doi.org/10.1021/ic201403k |*Inorg. Chem.* 2011, 50, 10342–10352

Table 4. Selected Interatomic Distances (Å) and Angles (deg) for Complex 3·MeOH·3H$_2$O

Ni1···Ni2	3.4752(10)	Ni1−N24	2.105(4)	Ni3−N13	2.097(4)	Ni5−O10	2.050(3)
Ni1···Ni5	3.4577(10)	Ni2−N7	2.025(4)	Ni3−N8	2.104(5)	Ni5−O8	2.057(3)
Ni2···Ni3	3.1973(11)	Ni2−O1	2.063(3)	Ni4−O8	2.031(3)	Ni5−N19	2.081(4)
Ni4···Ni5	3.1242(9)	Ni2−N6	2.070(4)	Ni4−N15	2.043(4)	Ni5−N24	2.112(4)
Mn1···Ni3	3.4232(11)	Ni2−N8	2.093(4)	Ni4−N18	2.067(4)	Mn1−O7	1.944(3)
Mn1···Ni4	3.4870(11)	Ni2−N3	2.094(4)	Ni4−N16	2.082(4)	Mn1−O4	1.963(3)
Ni1−N27	2.029(4)	Ni2−O3	2.101(3)	Ni4−N17	2.109(4)	Mn1−O6	1.970(3)
Ni1−N2	2.029(4)	Ni3−N12	2.029(4)	Ni4−N19	2.110(4)	Mn1−O3	1.987(3)
Ni1−N1	2.081(4)	Ni3−N11	2.072(6)	Ni5−N22	2.043(4)	Mn1−O8	2.137(3)
Ni1−N28	2.090(4)	Ni3−O3	2.086(3)	Ni5−N23	2.048(4)	Mn1−O5	2.140(3)
Ni1−N3	2.093(4)	Ni3−N14	2.092(4)				
N27−Ni1−N2	176.42(15)	N6−Ni2−O3	165.13(14)	O8−Ni4−N16	162.13(14)	N19−Ni5−N24	174.17(15)
N1−Ni1−N3	166.53(14)	N11−Ni3−O3	163.9(3)	N17−Ni4−N19	171.14(16)	O7−Mn1−O4	173.90(14)
N28−Ni1−N24	168.97(15)	N12−Ni3−N14	167.08(18)	N22−Ni5−O10	175.06(14)	O6−Mn1−O3	178.72(13)
N7−Ni2−O1	173.95(14)	N13−Ni3−N8	170.99(16)	N23−Ni5−O8	166.59(14)	O8−Mn1−O5	177.82(13)
N8−Ni2−N3	171.36(16)	N15−Ni4−N18	164.32(16)				

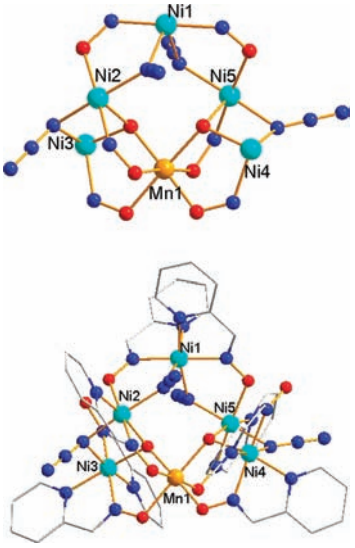

Figure 3. Representation of the complete $[MnNi_5(\mu\text{-}N_3)_4(\mu\text{-}OH)_2(\mu\text{-}ON)_6]^+$ core of **3** (top), and structure of the $[Mn^{III}Ni^{II}_5(N_3)_4(pao)_6(paoH)_2(\mu_3\text{-}OH)_2]^+$ cation (bottom). Color scheme: Mn, yellow; Ni, cyan; O, red; N, blue; C, gray; Cl, green. Hydrogen atoms have been omitted for clarity.

Table 5. Selected Interatomic Distances (Å) and Angles (deg) for Complex 4·2H$_2$O·6MeOH

Mn1−O1	1.878(3)	Ni1−O1	2.042(2)
Mn1−O3	1.894(3)	Ni1−N3	2.052(3)
Mn1−O6^a	1.941(3)	Ni1−N1	2.072(3)
Mn1−O2	1.992(2)	Ni1−N2	2.079(3)
Mn1−O4	2.237(3)	Ni1−N4	2.093(4)
Mn1−O2^a	2.329(2)	Ni1−O2	2.132(3)
O1−Mn1−O6^a	165.85(12)	N3−Ni1−N1	168.51(13)
O3−Mn1−O2	168.00(11)	O1−Ni1−N2	174.36(12)
O4−Mn1−O2^a	170.18(10)	N4−Ni1−O2	165.57(12)

^{a} $-x+1, -y, -z+2$.

To confirm the ground states and evaluate the magnitude of the ZFS parameter D for complexes **1**−**3**, magnetization data

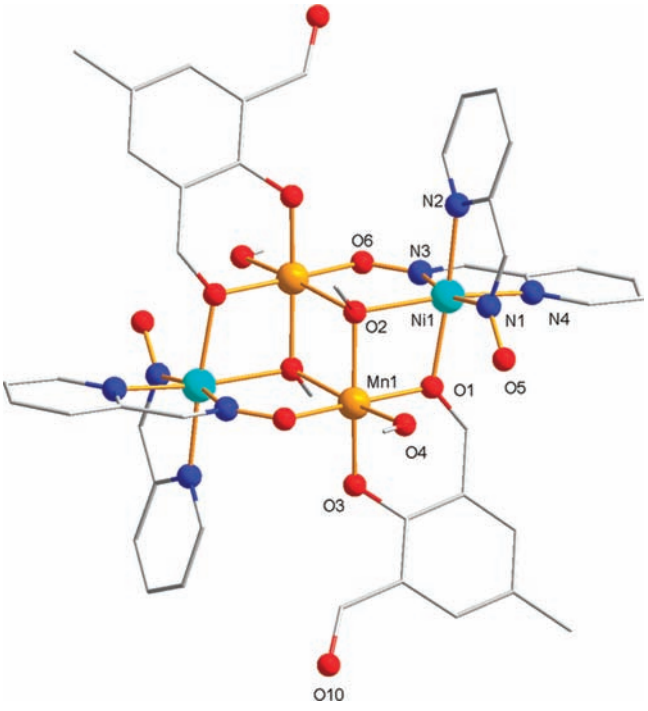

Figure 4. Structure of complex **4**. Color scheme: Mn, yellow; Ni, cyan; O, red; N, blue; C, gray. Hydrogen atoms have been omitted for clarity.

(M) were collected in the dc magnetic field range 0.1−5 T at 2.0−10 K. The data for complexes **1**, **2**, and **3** are shown in Figure 7 (top), Figure S1, Supporting Information, and Figure 7 (bottom) as reduced magnetization ($M/N\mu_B$) versus H/T plots. The data were fitted using the program ANISOFIT 2.0[26] by assuming only the spin ground state of the molecule is populated and the spin Hamiltonian employed to fit is $\hat{H} = D\hat{S}_z^2 + E(\hat{S}_x^2 + \hat{S}_y^2) + g_{iso}\mu_B S\cdot B$. The best fits are shown as the solid lines in Figure 7 with parameters $S = 5$, $g = 1.94$, and $D = -0.38$ cm^{-1} for **1** (using the data ≤2 T) and $S = 3$, $g = 2.05$, and $D = -0.86$ cm^{-1} for complex **3**. Alternative fits with $S = 4$ or 6 for complex **1** and $S = 2$ or 4 for complex **3** gave unreasonable values of g and D and thus were rejected. No satisfactory fit of the data was obtained for

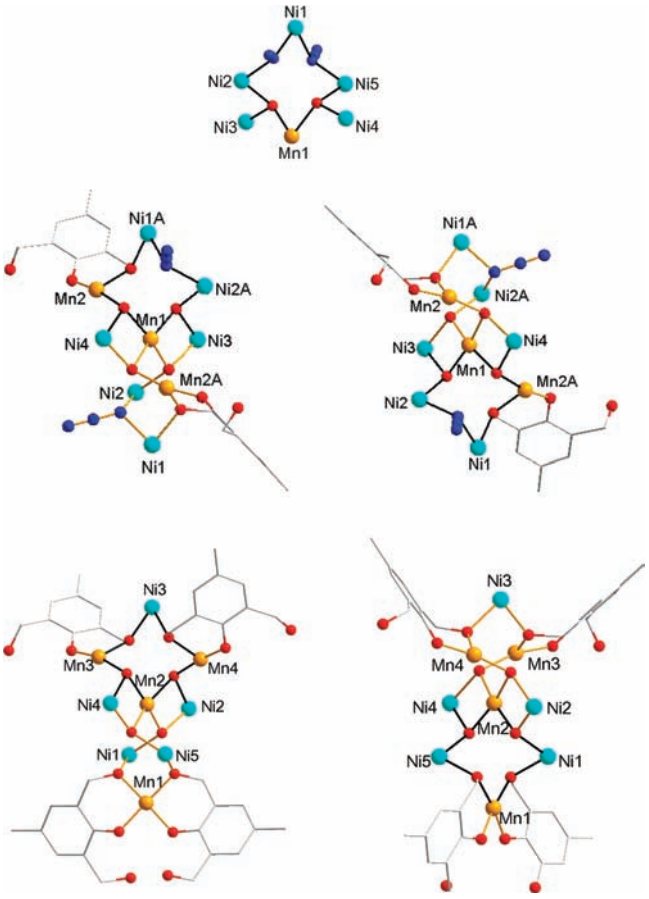

Figure 5. Comparison of the structures of **1**−**3**, emphasizing the common units of $[M_6(\mu_3\text{-OH})_2(\mu\text{-OR})_n(\mu\text{-N}_3)_{2-n}]$. (Top) Core of **3**, showing unit of $[MnNi_5(\mu_3\text{-OH})_2(\mu\text{-N}_3)_2]$. (Middle) Core of **2**, showing units of $[Mn_2Ni_4(\mu_3\text{-OH})_2(\mu\text{-OR})(\mu\text{-N}_3)]$. (Bottom) Core of **1**, showing units of $[Mn_3Ni_3(\mu_3\text{-OH})_2(\mu\text{-OR})_2]$ and $[Mn_2Ni_4(\mu\text{-OH})_2(\mu\text{-OR})_2]$. Color scheme: Mn, yellow; Ni, cyan; O, red; N, blue; C, gray. Oximate groups and hydrogen atoms have been omitted for clarity.

complex **2**, and a poorer quality fit was obtained for **1** using data up to 5 T, possibly due to population of low-lying excited states at low temperatures, which is a common problem in large clusters.[27]

For complex **4**, plots of $\chi_m T$ and χ_m vs T are shown in Figure 8 (top). The $\chi_m T$ value is 8.09 $cm^3\ K\ mol^{-1}$ at 300 K, close to the spin-only value (8.00 $cm^3\ K\ mol^{-1}$, $g = 2$) expected for two Mn^{III} and two Ni^{II} noninteracting ions. The $\chi_m T$ value gradually decreases with decreasing temperature to 0.75 $cm^3\ K\ mol^{-1}$ at 2 K, suggesting an overall antiferromagnetic interaction within the complex and an $S = 0$ ground-state spin. In order to determine the pairwise exchange interactions, the susceptibility data was fitted using the magnetism package MAGPACK[28] based on the interaction pattern (Figure 8, bottom) and the corresponding Hamiltonian (eq 1) from a temperature above 20 K[5e,25a] to avoid the influence of zero-field splitting.

$$\hat{H} = -2J_1(\hat{S}_1\hat{S}_4 + \hat{S}_2\hat{S}_3) - 2J_2(\hat{S}_1\hat{S}_2 + \hat{S}_3\hat{S}_4) - 2J_3\hat{S}_1\hat{S}_3 \quad (1)$$

The best-fit parameters obtained are $J_1 = -0.70\ cm^{-1}$, $J_2 = 8.50\ cm^{-1}$, $J_3 = -4.50\ cm^{-1}$, $g = 2.02$, and $R = 1.61 \times 10^{-5}$ (defined as $\Sigma[(\chi_m)_{calcd} - (\chi_m)_{obsd}]^2/\Sigma[(\chi_m)_{obsd}]^2$). The antiferromagnetic coupling (J_1) between Mn^{III} and Ni^{II} atoms via μ-methoxo-μ-oximato linkage is consistent with those found for the other Mn^{III} Ni^{II} complexes via oximato bridges,[8a,c,10b−e,13,29] although in a weaker strength, which may be attributed to the deviation of the structure. The ferromagnetic interaction (J_2) between Mn^{III} and Ni^{II} atoms via μ-methoxo-μ-alkoxo linkage is consistent with those for comparable exchange couplings.[5g,25a,b] In addition, the antiferromagnetic interaction (J_3) between the Mn^{III}

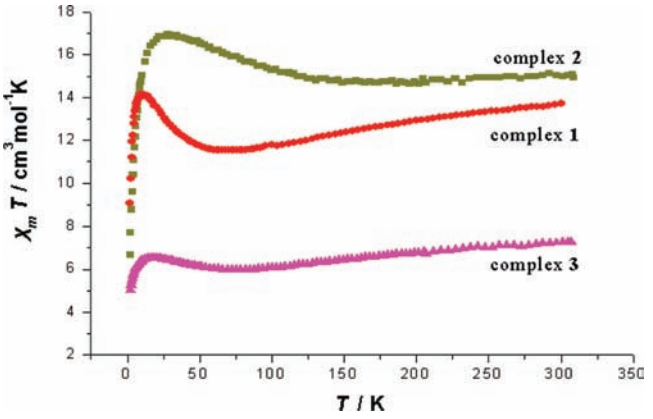

Figure 6. Plots of $\chi_m T$ vs T for complexes **1**−**3**.

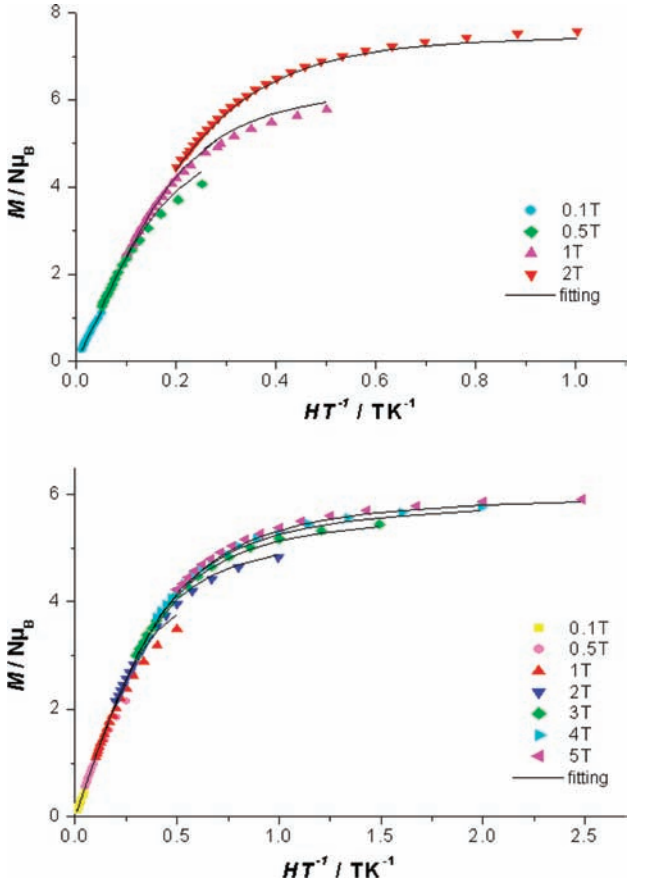

Figure 7. Plots of $M/N\mu_B$ vs H/T for complexes **1** (top) and **3** (bottom) at the indicated applied fields. Solid lines represent the best fits of the data.

dx.doi.org/10.1021/ic201403k |*Inorg. Chem.* 2011, 50, 10342–10352

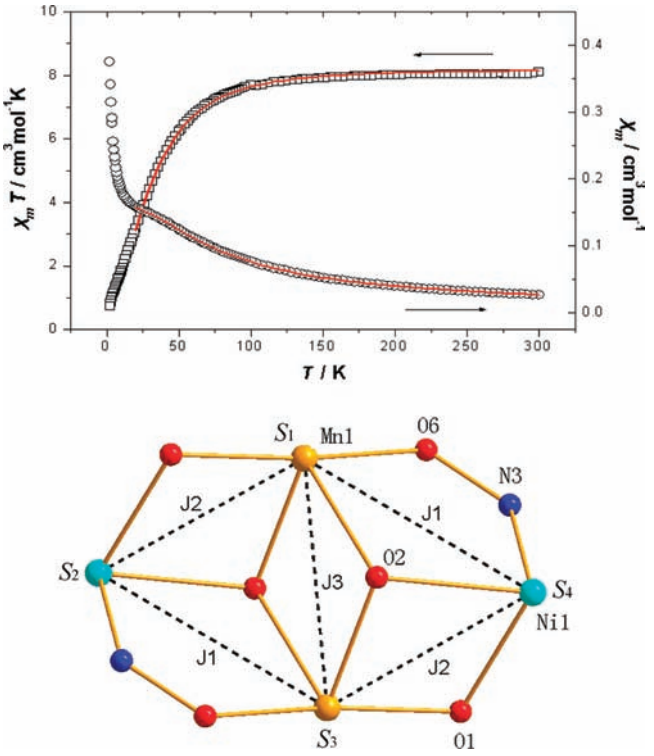

Figure 8. (Top) Plots of $\chi_m T$ (□) and χ_m (○) vs T for complex **4**. Solid lines represent the best-fit curves using the parameters described in the text. (Bottom) Spin topology for **4** assuming three different J values.

atoms is in agreement with those for other dimanganese(III) units with μ-methoxo bridging groups.[30]

Alternating Current Magnetic Susceptibility Studies. The ac susceptibility measurements were carried out on complexes **1**−**4** in the temperature range 2−15 K with a 3.0 G ac field oscillating at six frequencies between 311 and 2311 Hz. For **1**, the in-phase $\chi'_m T$ value increases slightly with decreasing temperature from 15 K, plateaus at ∼14.37 cm^3 mol^{-1} K in the 7.5−11 K region, and then decreases with decreasing temperature, where the lower temperature drops may be attributed to the intermolecular interactions and zero-field splitting (Figure 9, top). As described elsewhere, the in-phase ac susceptibility signal (χ'_m) is a useful way to determine the ground-state spin S of a molecular, since it can avoid the potential complications of measurements in an applied dc field.[4b,9i,27b,31] In this case, the $\chi'_m T$ value is almost temperature independent in the 7.5−11 K region and the value indicates an $S = 5$ ground state with $g < 2$, which is consistent with the determination from the dc magnetic susceptibility data. Below ∼2.5 K, **1** displays a frequency-dependent decrease in $\chi'_m T$ and concomitant appearance of out-of-phase χ''_m signals, indicating it may be a SMM with slow kinetics of magnetization reversal (Figure 9). The peaks of the χ''_m signals are located at temperatures well below 1.8 K.

To the best of our knowledge, only a small family of $Mn^{III}Ni^{II}$ SMMs has been reported to date. All of them are tetramers, including four distorted $Mn^{III}_3Ni^{II}$ cubanes[5e] with formula $[Mn^{III}_3Ni^{II}(hmp)_3O(N_3)_3(O_2CR)_3]$ (hmpH = pyridinemethanol), a linear-type $Mn^{III}_2Ni^{II}_2$ complex[10b] achieved by chemical modification of a known Mn^{III} Salen-type SMM, and the complex $[Mn^{III}_2Ni^{II}_2Cl_2(salpa)_2]$[5g] (salpa = *N*-(2-hydroxybenzyl)-3-amino-1-propanol) with an incomplete double-cube core.

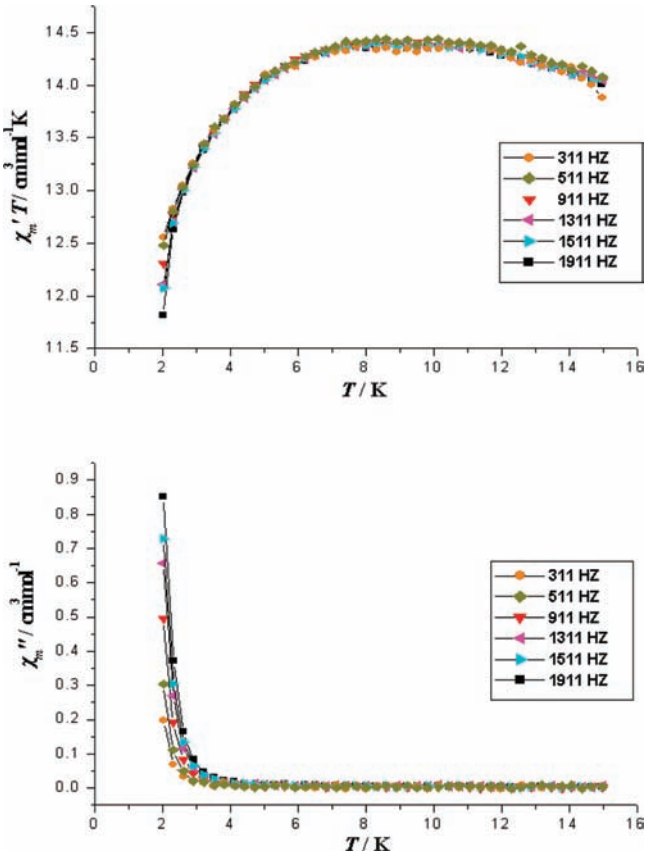

Figure 9. In-phase (χ'_m) (as $\chi'_m T$, top) and out-of-phase (χ''_m, bottom) ac susceptibility signals of complex **1** in a 3.0 G field oscillating at the indicated frequencies.

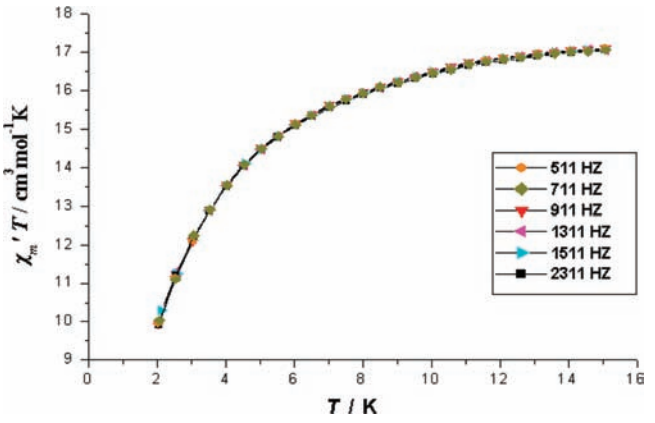

Figure 10. In-phase (χ'_m) (as $\chi'_m T$) ac susceptibility signal of complex **2** in a 3.0 G field oscillating at the indicated frequencies.

For **2**, the in-phase $\chi'_m T$ value decreases slowly below 15 K (Figure 10), indicating depopulation of excited states with S greater than that of the ground state, and extrapolation of the plot to 0 K from the high-temperature linear section gives a value of approximately 15.37 cm^3 mol^{-1} K, which suggests an $S = 5$ ground state with $g > 2$, consistent with the determination from the dc magnetic susceptibility data.

For **3**, the in-phase $\chi'_m T$ value is almost temperature independent in the 13−15 K region and decreases gradually to 2 K

dx.doi.org/10.1021/ic201403k |*Inorg. Chem.* 2011, 50, 10342–10352

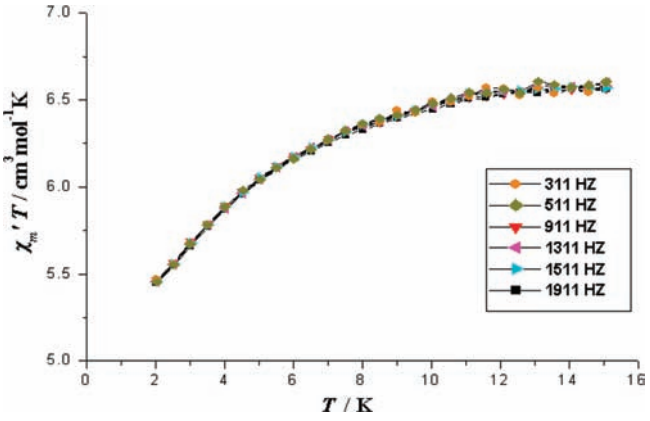

Figure 11. In-phase (χ'_m) (as χ'_mT) ac susceptibility signal of complex **3** in a 3.0 G field oscillating at the indicated frequencies.

(Figure 11). Extrapolation of the high-temperature linear section of the χ'_mT plot to 0 K gives a value of approximately 6.35 cm^3 mol^{-1} K, which suggests an $S = 3$ ground state with $g > 2$, in agreement with the determination from the dc magnetic susceptibility data.

For **4**, the ac in-phase χ'_mT versus T data (Figure S2, Supporting Information) steadily decreases below 15 K and heads for approximately 0 cm^3 mol^{-1} K at 0 K, which supports an $S = 0$ ground-state spin.

No out-of-phase ac signal is observed for complexes **2**−**4**.

CONCLUSIONS

Use of "metal oximate" ligand $[Ni(paoH)_2Cl_2]$ with the coligands $hmcH_3$ and/or NaN_3 in a reaction system involving the simple Mn(II) reagents affords a family of heterometallic Mn^{III}/Ni^{II} clusters with various nuclearities. Complexes **1** and **2** represent the first heterometallic nonanuclear metal/oxime clusters as well as the largest 3d heterometal/oxime clusters discovered to date. Complexes **1**−**3** contain similar units of $[M_6(\mu_3\text{-}OH)_2(\mu\text{-}OR)_n(\mu\text{-}N_3)_{2-n}]$, which differ in Mn/Ni ratio and the presence of the coligands $hmcH^{2-}$ and/or N_3^-. The deviation of the structures indicates the influence of the coligands on the assembly of the clusters, which may originate from the different affinity of the metal atoms to the O donors or N donors. The same reaction carried out in DMF gives a nanonuclear complex **1** while in MeOH yields a completely different tetranuclear **4**, suggesting the solvent dependence of the reaction products.

The magnetic susceptibility study of **1**−**3** indicates a mixture of both ferro- and antiferromagnetic exchange interactions within the complexes, which is consistent with the presence of the bridging end-on azide groups/alkoxide groups and OH^-/oximate groups. **1** exhibits out-of-phase ac susceptibility signals, indicating it may be a SMM, while **2**−**4** do not exhibit out-of-phase ac susceptibility signal. For **4**, the couplings via different pathways between Mn^{III} and Ni^{II} ions as well as between Mn^{III} ions have been evaluated based on a 3-J model.

The synthetic methodology described in this work is now being extended, and several other oximate-based metalloligands or coligands are being introduced to the system to construct novel heterometallic complexes with interesting architectures and magnetic properties.

ASSOCIATED CONTENT

Supporting Information. X-ray crystallographic data for complexes **1**−**4** in CIF format and Figures S1 and S2. This material is available free of charge via the Internet at http://pubs.acs.org.

AUTHOR INFORMATION

Corresponding Author
*Fax: (+86) 0591-83792395. E-mail: ccn@fjirsm.ac.cn.

ACKNOWLEDGMENT

This work was supported by the National Natural Science Foundation of China (Nos. 20973172, 21071145, and 21173219) and the National Basic Research Program of China (No. 2009CB220009).

REFERENCES

(1) (a) Holm, R. H.; Kennepohl, P.; Solomon, E. I. *Chem. Rev.* **1996**, *96*, 2239. (b) Wu, A. J.; Penner-Hahn, J. E.; Pecoraro, V. L. *Chem. Rev.* **2004**, *104*, 903. (c) Rao, P. V.; Holm, R. H. *Chem. Rev.* **2004**, *104*, 527. (d) *Manganese Redox Enzymes*; VCH Publishers: New York, 1992.

(2) Kahn, O. *Molecular Magnetism*; VCH: New York, 1993.

(3) (a) Sessoli, R.; Gatteschi, D.; Caneschi, A.; Novak, M. A. *Nature* **1993**, *365*, 141. (b) Sessoli, R.; Tsai, H. L.; Schake, A. R.; Wang, S. Y.; Vincent, J. B.; Folting, K.; Gatteschi, D.; Christou, G.; Hendrickson, D. N. *J. Am. Chem. Soc.* **1993**, *115*, 1804. (c) Christou, G.; Gatteschi, D.; Hendrickson, D. N.; Sessoli, R. *MRS Bull.* **2000**, *25*, 66. (d) Gatteschi, D.; Sessoli, R. *Angew. Chem., Int. Ed.* **2003**, *42*, 268. (e) Aromi, G.; Brechin, E. K. *Stuct. Bonding* 2006, *122*, 1.

(4) (a) Wittick, L. M.; Murray, K. S.; Moubaraki, B.; Batten, S. R.; Spiccia, L.; Berry, K. J. *Dalton Trans.* **2004**, 1003. (b) Murugesu, M.; Raftery, J.; Wernsdorfer, W.; Christou, G.; Brechin, E. K. *Inorg. Chem.* **2004**, *43*, 4203. (c) Soler, M.; Wernsdorfer, W.; Folting, K.; Pink, M.; Christou, G. *J. Am. Chem. Soc.* **2004**, *126*, 2156. (d) Sanudo, E. C.; Wernsdorfer, W.; Abboud, K. A.; Christou, G. *Inorg. Chem.* **2004**, *43*, 4137. (e) Murugesu, M.; Habrych, M.; Wernsdorfer, W.; Abboud, K. A.; Christou, G. *J. Am. Chem. Soc.* **2004**, *126*, 4766. (f) Tasiopoulos, A. J.; Vinslava, A.; Wernsdorfer, W.; Abboud, K. A.; Christou, G. *Angew. Chem., Int. Ed.* **2004**, *43*, 2117. (g) Miyasaka, H.; Clerac, R.; Wernsdorfer, W.; Lecren, L.; Bonhomme, C.; Sugiura, K.; Yamashita, M. *Angew. Chem., Int. Ed.* **2004**, *43*, 2801. (h) Boskovic, C.; Bircher, R.; Tregenna-Piggott, P. L. W.; Gudel, H. U.; Paulsen, C.; Wernsdorfer, W.; Barra, A. L.; Khatsko, E.; Neels, A.; Stoeckli-Evans, H. *J. Am. Chem. Soc.* **2003**, *125*, 14046. (i) Brechin, E. K.; Soler, M.; Davidson, J.; Hendrickson, D. N.; Parsons, S.; Christou, G. *Chem. Commun.* **2002**, 2252. (j) Boskovic, C.; Brechin, E. K.; Streib, W. E.; Folting, K.; Bollinger, J. C.; Hendrickson, D. N.; Christou, G. *J. Am. Chem. Soc.* **2002**, *124*, 3725. (k) Aubin, S. M. J.; Wemple, M. W.; Adams, D. M.; Tsai, H.-L.; Christou, G.; Hendrickson, D. N. *J. Am. Chem. Soc.* **1996**, *118*, 7746. (l) Yoo, J.; Brechin, E. K.; Yamaguchi, A.; Nakano, M.; Huffman, J. C.; Maniero, A. L.; Brunel, L. C.; Awaga, K.; Ishimoto, H.; Christou, G.; Hendrickson, D. N. *Inorg. Chem.* **2000**, *39*, 3615.

(5) (a) Zaleski, C. M.; Depperman, E. C.; Kampf, J. W.; Kirk, M. L.; Pecoraro, V. L. *Angew. Chem., Int. Ed.* **2004**, *43*, 3912. (b) Sokol, J. J.; Hee, A. G.; Long, J. R. *J. Am. Chem. Soc.* **2002**, *124*, 7656. (c) Karasawa, S.; Zhou, G. Y.; Morikawa, H.; Koga, N. *J. Am. Chem. Soc.* **2003**, *125*, 13676. (d) Martinez-Lillo, J.; Armentano, D.; De Munno, G.; Wernsdorfer, W.; Clemente-Juan, J. M.; Krzystek, J.; Lloret, F.; Julve, M.; Faus, J. *Inorg. Chem.* **2009**, *48*, 3027. (e) Feng, P. L.; Beedle, C. C.; Koo, C.; Wernsdorfer, W.; Nakano, M.; Hill, S.; Hendrickson, D. N. *Inorg. Chem.* **2008**, *47*, 3188. (f) Oshio, H.; Nihei, M.; Yoshida, A.; Nojiri, H.; Nakano, M.; Yamaguchi, A.; Karaki, Y.; Ishimoto, H. *Chem.—Eur. J.* **2005**, *11*, 843. (g) Oshio, H.; Nihei, M.; Koizumi, S.; Shiga, T.; Nojiri,

H.; Nakano, M.; Shirakawa, N.; Akatsu, M. *J. Am. Chem. Soc.* **2005**, *127*, 4568. (h) Osa, S.; Kido, T.; Matsumoto, N.; Re, N.; Pochaba, A.; Mrozinski, J. *J. Am. Chem. Soc.* **2004**, *126*, 420.

(6) (a) Chaudhuri, P. *Coord. Chem. Rev.* **2003**, *243*, 143. (b) Milios, C. J.; Stamatatos, T. C.; Perlepes, S. P. *Polyhedron* **2006**, *25*, 134. (c) Smith, A. G.; Tasker, P. A.; White, D. J. *Coord. Chem. Rev.* **2003**, *241*, 61.

(7) Milios, C. J.; Raptopoulou, C. P.; Terzis, A.; Lloret, F.; Vicente, R.; Perlepes, S. P.; Escuer, A. *Angew. Chem., Int. Ed.* **2004**, *43*, 210.

(8) (a) Clerac, R.; Miyasaka, H.; Yamashita, M.; Coulon, C. *J. Am. Chem. Soc.* **2002**, *124*, 12837. (b) Miyasaka, H.; Saitoh, A.; Yamashita, M.; Clerac, R. *Dalton Trans.* **2008**, 2422. (c) Miyasaka, H.; Clerac, R.; Mizushima, K.; Sugiura, K.; Yamashita, M.; Wernsdorfer, W.; Coulon, C. *Inorg. Chem.* **2003**, *42*, 8203.

(9) (a) Biswas, B.; Pieper, U.; Weyhermuller, T.; Chaudhuri, P. *Inorg. Chem.* **2009**, *48*, 6781. (b) Karotsis, G.; Stoumpos, C.; Collins, A.; White, F.; Parsons, S.; Slawin, A. M. Z.; Papaefstathiou, G. S.; Brechin, E. K. *Dalton Trans.* **2009**, 3388. (c) Stamatatos, T. C.; Diamantopoulou, E.; Raptopoulou, C. P.; Psycharis, V.; Escuer, A.; Perlepes, S. P. *Inorg. Chem.* **2007**, *46*, 2350. (d) Stamatatos, T. C.; Escuer, A.; Abboud, K. A.; Raptopoulou, C. P.; Perlepes, S. P.; Christou, G. *Inorg. Chem.* **2008**, *47*, 11825. (e) Afrati, T.; Zaleski, C. M.; Dendrinou-Samara, C.; Mezei, G.; Kampf, J. W.; Pecoraro, V. L.; Kessissoglou, D. P. *Dalton Trans.* **2007**, 2658. (f) Milios, C. J.; Inglis, R.; Vinslava, A.; Bagai, R.; Wernsdorfer, W.; Parsons, S.; Perlepes, S. P.; Christou, G.; Brechin, E. K. *J. Am. Chem. Soc.* **2007**, *129*, 12505. (g) Milios, C. J.; Inglis, R.; Vinslava, A.; Prescimone, A.; Parsons, S.; Perlepes, S. P.; Christou, G.; Brechin, E. K. *Chem. Commun.* **2007**, 2738. (h) Yang, C. I.; Wernsdorfer, W.; Lee, G. H.; Tsai, H. L. *J. Am. Chem. Soc.* **2007**, *129*, 456. (i) Stamatatos, T. C.; Foguet-Albiol, D.; Lee, S. C.; Stoumpos, C. C.; Raptopoulou, C. P.; Terzis, A.; Wernsdorfer, W.; Hill, S. O.; Perlepes, S. P.; Christou, G. *J. Am. Chem. Soc.* **2007**, *129*, 9484. (j) Pathmalingam, T.; Gorelsky, S. I.; Burchell, T. J.; Bedard, A. C.; Beauchemin, A. M.; Clerac, R.; Murugesu, M. *Chem. Commun.* **2008**, 2782. (k) Inglis, R.; Jones, L. F.; Mason, K.; Collins, A.; Moggach, S. A.; Parsons, S.; Perlepes, S. P.; Wernsdorfer, W.; Brechin, E. K. *Chem.—Eur. J.* **2008**, *14*, 9117.

(10) (a) Khanra, S.; Biswas, B.; Golze, C.; Buchner, B.; Kataev, V.; Weyhermuller, T.; Chaudhuri, P. *Dalton Trans.* **2007**, 481. (b) Kachi-Terajima, C.; Miyasaka, H.; Saitoh, A.; Shirakawa, N.; Yamashita, M.; Clerac, R. *Inorg. Chem.* **2007**, *46*, 5861. (c) Chaudhuri, P.; Weyhermuller, T.; Wagner, R.; Khanra, S.; Biswas, B.; Bothe, E.; Bill, E. *Inorg. Chem.* **2007**, *46*, 9003. (d) Miyasaka, H.; Nezu, T.; Sugimoto, K.; Sugiura, K.; Yamashita, M.; Clerac, R. *Chem.—Eur. J.* **2005**, *11*, 1592. (e) Miyasaka, H.; Nezu, T.; Sugimoto, K.; Sugiura, K. C.; Yamashita, M.; Clerac, R. *Inorg. Chem.* **2004**, *43*, 5486. (f) Miyasaka, H.; Nezu, T.; Iwahori, F.; Furukawa, S.; Sugimoto, K.; Clerac, R.; Sugiura, K.; Yamashita, M. *Inorg. Chem.* **2003**, *42*, 4501. (g) Ross, S.; Weyhermuller, T.; Bill, E.; Wieghardt, K.; Chaudhuri, P. *Inorg. Chem.* **2001**, *40*, 6656.

(11) Pal, S.; Mukherjee, R.; Tomas, M.; Falvello, L. R.; Chakravorty, A. *Inorg. Chem.* **1986**, *25*, 200.

(12) Birkelbach, F.; Winter, M.; Floerke, U.; Haupt, H.-J.; Butzlaff, C.; Lengen, M.; Bill, E.; Trautwein, A. X.; Wieghardt, K.; Chaudhuri, P. *Inorg. Chem.* **1994**, *33*, 3990.

(13) Weyhermuller, T.; Wagner, R.; Khanra, S.; Chaudhuri, P. *Dalton Trans.* **2005**, 2539.

(14) Khanra, S.; Uller, T. W.; Chaudhuri, P. *Dalton Trans.* **2007**, 4675.

(15) Krause, R. A.; Busch, D. H. *J. Am. Chem. Soc.* **1960**, *82*, 4830.

(16) (a) Lampropoulos, C.; Abboud, K. A.; Stamatatos, T. C.; Christou, G. *Inorg. Chem.* **2009**, *48*, 813. (b) Ako, A. M.; Mereacre, V.; Clerac, R.; Wernsdorfer, W.; Hewitt, I. J.; Anson, C. E.; Powell, A. K. *Chem. Commun.* **2009**, 544. (c) Ako, A. M.; Hewitt, I. J.; Mereacre, V.; Clerac, R.; Wernsdorfer, W.; Anson, C. E.; Powell, A. K. *Angew. Chem., Int. Ed.* **2006**, *45*, 4926. (d) Yang, C. I.; Lee, G. H.; Wur, C. S.; Lin, J. G.; Tsai, H. L. *Polyhedron* **2005**, *24*, 2215.

(17) Sheldrick, G. M. *SADABS: Program for Siemens Area Detector Absorption Corrections*; University of Göttingen: Germany, 1997.

(18) Sheldrick, G. M. *SHELXTL-97*, 5.0th ed.; Siemens Analytical X-ray Instruments Inc.: Madison, WI, 1997.

(19) Van der sluis, P.; Spek, A. L. *Acta Crystallogr., Sect. A: Found. Crystallogr.* **1990**, *46*, 194.

(20) Liu, W. T.; Thorp, H. H. *Inorg. Chem.* **1993**, *32*, 4102.

(21) (a) Pajunen, A.; Mutikainen, I.; Saarinen, H.; Orama, M. *Z. Kristallogr., New Cryst. Struct.* **1999**, *214*, 217. (b) Stamatatos, T. C.; Diamantopoulou, E.; Tasiopoulos, A.; Psycharis, V.; Vicente, R.; Raptopoulou, C. P.; NastopouloS, V.; Escuer, A.; Perlepes, S. P. *Inorg. Chim. Acta* **2006**, *359*, 4149. (c) Khanra, S.; Weyhermuller, T.; Rentschler, E.; Chaudhuri, P. *Inorg. Chem.* **2005**, *44*, 8176.

(22) Roubeau, O.; Lecren, L.; Li, Y. G.; Le Goff, X. F.; Clerac, R. *Inorg. Chem. Commun.* **2005**, *8*, 314.

(23) Gavrilenko, K. S.; Punln, S. V.; Cador, O.; Golhen, S.; Ouahab, L.; Pavlishchuk, V. V. *Inorg. Chem.* **2005**, *44*, 5903.

(24) (a) Hiraga, H.; Miyasaka, H.; Clerac, R.; Fourmigue, M.; Yamashita, M. *Inorg. Chem.* **2009**, *48*, 2887. (b) Kachi-Terajima, C.; Miyasaka, H.; Saitoh, A.; Shirakawa, N.; Yamashita, M.; Clerac, R. *Inorg. Chem.* **2007**, *46*, 5861.

(25) (a) Nihei, M.; Yoshida, A.; Koizumi, S.; Oshio, H. *Polyhedron* **2007**, *26*, 1997. (b) Koikawa, M.; Ohba, M.; Tokii, T. *Polyhedron* **2005**, *24*, 2257. (c) Sunatsuki, Y.; Shimada, H.; Matsuo, T.; Nakamura, M.; Kai, F.; Matsumoto, N.; Re, N. *Inorg. Chem.* **1998**, *37*, 5566.

(26) Shores, M. P.; Sokol, J. J.; Long, J. R. *J. Am. Chem. Soc.* **2002**, *124*, 2279.

(27) (a) Milios, C. J.; Manoli, M.; Rajaraman, G.; Mishra, A.; Budd, L. E.; White, F.; Parsons, S.; Wernsdorfer, W.; Christou, G.; Brechin, E. K. *Inorg. Chem.* **2006**, *45*, 6782. (b) Tasiopoulos, A. J.; Wernsdorfer, W.; Abboud, K. A.; Christou, G. *Inorg. Chem.* **2005**, *44*, 6324.

(28) (a) Borras-Almenar, J. J.; Clemente-Juan, J. M.; Coronado, E.; Tsukerblat, B. S. *J. Comput. Chem.* **2001**, *22*, 985. (b) Borras-Almenar, J. J.; Clemente-Juan, J. M.; Coronado, E.; Tsukerblat, B. S. *Inorg. Chem.* **1999**, *38*, 6081.

(29) (a) Saitoh, A.; Miyasaka, H.; Yamashita, M.; Clerac, R. *J. Mater. Chem.* **2007**, *17*, 2002. (b) Birkelbach, F.; Florke, U.; Haupt, H. J.; Butzlaff, C.; Trautwein, A. X.; Wieghardt, K.; Chaudhuri, P. *Inorg. Chem.* **1998**, *37*, 2000.

(30) (a) Lan, Y.; Novitchi, G.; Clerac, R.; Tang, J. K.; Madhu, N. T.; Hewitt, I. J.; Anson, C. E.; Brooker, S.; Powell, A. K. *Dalton Trans.* **2009**, 1721. (b) Paine, T. K.; Weyhermuller, T.; Bothe, E.; Wieghardt, K.; Chaudhuri, P. *Dalton Trans.* **2003**, 3136. (c) Abbati, G. L.; Cornia, A.; Fabretti, A. C.; Caneschi, A.; Gatteschi, D. *Inorg. Chem.* **1998**, *37*, 3759.

(31) (a) Wang, M.; Ma, C. B.; Wen, H. M.; Chen, C. N. *Dalton Trans.* **2009**, 994. (b) Ma, Y. S.; Song, Y.; Li, Y. Z.; Zheng, L. M. *Inorg. Chem.* **2007**, *46*, 5459.